Stability of Synergistic Behavior in Ethyl Cellulose-Glycerol Monostearate Binary Oleogels

Current Research in Food Science 12 (2026) 101421

Contents lists available at ScienceDirect

Current Research in Food Science

journal homepage: www.sciencedirect.com/journal/current-research-in-food-science

Stability of synergistic behavior in ethyl cellulose-glycerol monostearate binary oleogels

Mursalin Sajib [a,b], Nitin Nitin [a,c], Andrew J. Gravelle [a,*]

[a] Department of Food Science and Technology, University of California, Davis, CA, USA
[b] Department of Life Sciences-Food and Nutrition Science, Chalmers University of Technology, Gothenburg, Sweden
[c] Department of Biological and Agricultural Engineering, University of California, Davis, CA, USA

ARTICLE INFO

Keywords:
Fat mimetics
Ethyl cellulose
Monoglyceride
Binary oleogel
Synergy
Storage stability
Polymorphic transition

ABSTRACT

This study investigates how synergistic interactions between ethyl cellulose (EC) and glycerol monostearate (GMS) govern the mechanical stability of binary oleogels during storage. Over 14 days at 22 °C, single-component GMS oleogels underwent a polymorphic transition from the metastable sub-α to the more stable β form, resulting in a pronounced loss of mechanical strength. In contrast, the extent of this transition in EC-GMS binary systems depended on whether the EC concentration was below, at, or above its critical gelation concentration (CGC), the threshold required to form a self-supporting polymer network. Formulations prepared with EC below its CGC (e.g., 2% EC) exhibited a significant reduction in hardness during storage, whereas those containing EC at or above its CGC maintained their synergistic enhancement in gel strength, attributable to a delayed GMS polymorphic transition. Moreover, preservation of this synergistic effect was governed by the EC/GMS ratio. When EC was used at its CGC (6%), at least 10% GMS was required to sustain gel strength over time. Increasing EC concentration also produced a greater shift in the GMS O–H stretching bands prior to storage, but was not observed after the polymorphic transition, thus demonstrating the direct contribution of hydrogen bonding to the synergistic behavior of the binary oleogels. Collectively, these findings provide a mechanistic basis for leveraging EC-GMS synergy to design physically stable oleogels with reduced total gelator concentration, thereby enabling the development of cost-effective and functional fat mimetics.

1. Introduction

Oleogels are emerging as promising alternatives to conventional solid fats, driven by health concerns over trans and saturated fat consumption, as well as considerations of environmental sustainability and animal welfare (Sivakanthan et al., 2022; Zhang et al., 2025). Their use has been explored across a broad range of food products, including baked goods (Giacomozzi et al., 2018), fat spreads (Palla et al., 2017), ground cooked salami (Woern et al., 2021), and adipose tissue mimetics (Soleimanian et al., 2024). Oleogels are typically categorized as having a majority liquid oil phase (typically ≥80%) stabilized within a gel-like matrix using one or more structuring agents other than crystalline triglycerides. Although a variety of approaches have been developed, the oleogelation process most commonly involves heating the oil-structurant mixture above the melting point or glass transition temperature of the oleogelator(s), followed by cooling to form a self-assembled three-dimensional network (Gravelle, 2024; Palla et al., 2022).

When select oleogelators are used in combination, cooperative or synergistic interactions may occur, offering significant advantages over using a single oleogelator (Sivakanthan et al., 2022). Such synergy allows oleogelators to be used at lower concentrations, while still enhancing the mechanical properties of the gel (Hu et al., 2025; Sajib et al., 2026). This provides greater formulation flexibility by combining the complementary properties of different structuring agents, enabling more precise tailoring of functional properties for specific food applications.

To date, many multi-component oleogelator systems have been explored, imparting various changes to the performance characteristics of the resulting oleogel (Pakseresht and Mazaheri Tehrani, 2022). One notable example is the combination of the polymeric oleogelator ethyl cellulose (EC) and the small-molecule crystalline oleogelator glycerol monostearate (GMS) (Davidovich-Pinhas et al., 2015; García-Ortega et al., 2024; Ji and Gravelle, 2025; Lopez-Martínez et al., 2015; Wang et al., 2026). While it is well established that combining these

* Corresponding author.
E-mail address: agravelle@ucdavis.edu (A.J. Gravelle).

https://doi.org/10.1016/j.crfs.2026.101421
Received 7 December 2025; Received in revised form 25 April 2026; Accepted 27 April 2026
Available online 28 April 2026

List of abbreviations

EC	ethyl cellulose
EC45	45 cP ethyl cellulose
FTIR	Fourier transform infrared
GMS	glycerol monostearate
CGC	critical gelling concentration
PLM	polarized light microscopy
DSC	differential scanning calorimetry
XRD	x-ray diffraction
G'	storage modulus
G"	loss modulus

compounds can dramatically enhance oleogel strength, little work has been done to systematically evaluate how the interactions between these molecules contribute to gel structuring. To this end, a recent study from our group comprehensively investigated the cooperative interactions between EC and GMS, conclusively demonstrating the synergistic nature of their structuring behavior (Sajib et al., 2026). This work showed that combining either low- or high-molecular-weight EC (10 cP EC and 45 cP EC, respectively) with GMS could produce a multiplicative increase in oleogel firmness compared to equivalent concentrations of their respective single-component oleogels. Furthermore, while incorporating EC below its critical gelation concentration (CGC) enhanced gel strength, the strongest synergistic effects were observed when both gelators were used at or above their respective CGCs, allowing each component to form a self-supporting network. Here, the CGC is defined as the minimum gelator concentration to form a self-supporting structure, and has been reported as ~6 wt% for 45 cP EC (EC45) (Zetzl et al., 2012) and ~2 wt% for GMS (García-Ortega et al., 2024). The increase in firmness was attributed to hydrogen bonding interactions between EC and GMS and further supported by GMS crystallization both along the EC polymer backbone and throughout the entrapped oil phase. These interactions also promoted nucleation of GMS and altered the morphology and organization of the resulting crystal network.

Single-component GMS oleogels are known to weaken over time due to polymorphic transitions from the sub-α to β phases, which lead to reduced hardness and oil-binding properties caused by β-crystal aggregation (Li et al., 2021; Li et al., 2024). This transition may also compromise the physical stability of GMS-containing binary oleogels. Therefore, in addition to characterizing the synergistic effects between EC and GMS in binary oleogelator systems, it is essential to assess their stability over time, since oleogels (and the food products formulated with them) must maintain structural integrity and functional performance throughout storage, transport, and shelf life. Although data on the storage stability of EC-GMS systems remain limited, existing studies suggest that combining oleogelators can mitigate the instability of individual components (Sivakanthan et al., 2022). For example, Bin Sintang et al. (2017) showed that combining palm oil-derived monoglycerides with phytosterol in a binary oleogelator system improved stability of monoglyceride during storage. Similarly, Lopez-Martínez et al. (2015) reported improved stability of monoglyceride-based oleogels in the presence of 6% 4 cP EC. Li et al. (2024) evaluated the effect of hydroxylated monoglycerides on both the gel strength and performance over extended storage times, but found high concentrations of these additives were required (20-40%) to retain gel strength. To date, however, no study has directly investigated the stability of the cooperative interaction between EC and GMS in binary oleogels upon storage. As a result, the extent to which GMS polymorphic transitions influence its structuring capacity and gelator efficiency, and how these changes affect the long-term performance of EC and GMS oleogels, remains unclear. This study therefore aimed to identify the key compositional factors influencing the retention and long-term persistence of their synergistic structuring behavior.

2. Materials and methods

2.1. Materials

EC45 (45 cP; ethoxy content 48–49.5%, per manufacturer specifications) and the antioxidant tert-butylhydroquinone (TBHQ, 97% purity) were obtained from Sigma Aldrich (Saint Louis, MO, USA). Distilled monoglycerides derived from hydrogenated soybean oil (GMS) was generously supplied by International Flavors & Fragrances (IFF), Inc. (Saint Louis, MO, USA). The GMS had a monoester content of ≥90%, according to the manufacturer specifications. A single lot of canola oil was purchased from a local retailer.

2.2. Oleogel sample preparation

To minimize variability in sample preparation, stock solutions (10% w/w; relative to oil) of EC oleogels were prepared in 400 g batch size by mixing EC with canola oil and 100 ppm TBHQ. The mixtures were heated on a hotplate to 160 °C with continuous stirring and held at this temperature for 10 min. After heating, the solutions were allowed to cool undisturbed at ambient temperature (~22 °C) overnight. CGC values of EC45 and GMS were confirmed to be consistent with published values using mechanical deformation testing, in which oleogels exceed a minimum trigger force at the point of penetration (see Section 2.3; data not shown).

To assess the stability of EC-GMS synergistic effects during storage, oleogels containing various concentrations of EC (0–10 wt% relative to the oil phase) and GMS (0–24 wt%; relative to the oil phase) were prepared. EC stock gel (10%) was combined with the required amount of GMS and canola oil in 20 ml glass scintillation vials (~15 g total sample). The mixtures were then heated in a forced-air convection oven (BINDER Inc., Bohemia, NY, USA) at 160 °C for 20 min, followed by manual mixing for ~5 s by repeated inversion of the capped vials (~10 inversions). After mixing, the vials were returned to the oven for an additional 10 min to ensure full dissolution of the oleogelators. The vials were then allowed to cool at ambient temperature overnight prior to further testing. Oleogels used for stability tests were stored in a temperature-controlled environment (22 °C) in the dark. The storage stability of the oleogels was assessed through a 14-day storage period (unless otherwise stated), as described in subsequent sections.

2.3. Large deformation mechanical analysis

Changes in the mechanical properties of the oleogels were assessed via a puncture test conducted using a TA.XTPlus Texture Analyzer (Stable Micro Systems, Scarsdale, NY, USA), following a method described by Ji and Gravelle (2025). The Texture Analyzer was equipped with either a 5 kg or 50 kg load cell and fitted with an 11 mm cylindrical stainless-steel probe with a rounded tip (TA-212). The test was performed using a crosshead speed of 1 mm/s and a penetration depth of 20 mm. Force–deformation data were collected using the Exponent Connect Software (version 8.1.2.0). Hardness was defined as the average force measured between 15 and 20 mm of penetration, calculated using a simple linear regression, as described by Ji and Gravelle (2025).

2.4. Microstructure of oleogel

Microstructural changes in the oleogels during storage were examined using an Olympus BX 50 optical microscope (Olympus Corporation, Tokyo, Japan) under polarized light. For sample preparation, ~5 mg of oleogel was placed on a glass slide and melted in a pre-heated oven at 160 °C for 20 min. A cover slip was then gently placed over the molten sample, followed by an additional 10-min heating period. The slides were then cooled to ambient temperature and stored in the dark for 1

and 14 days before imaging. Microscopy images were captured with a digital camera (Industrial Digital Camera, Sony Exmor CMOS Sensor, Sony Group, Japan) using the ToupView software (ToupTek Photonics, Hangzhou, Zhejiang, China). After imaging on Day 1, the prepared microscope slides were stored in a temperature-controlled environment (22 °C) in the dark prior to re-imaging.

2.5. Differential scanning calorimetry

The thermal behavior of the oleogels were examined using a differential scanning calorimeter (DSC 250, TA Instruments, New Castle, DE, USA). Approximately 10 mg of each sample was hermetically sealed in a 40 μl aluminum pan with an aluminum lid. The thermal protocol consisted of a three-stage cycle – first heating, cooling, and a second heating – conducted over a temperature range of 20 °C to 90 °C at 5 °C/min (Haj Eisa et al., 2020). A 3-min isothermal hold period was included between each transition step. The peak melting temperature (T_m) and the change in enthalpy (ΔH) for each thermal event were analyzed using TRIOS software (version 5, TA Instruments). All oleogels were evaluated on Day 1 and 14. Data from the second heating cycle of the DSC thermal protocol were used to represent Day 0, as this cycle reflects the thermal behavior of the oleogels immediately after preparation, without prolonged storage.

2.6. FTIR

The chemical functional groups present in oleogels were characterized using Fourier transform infrared (FTIR) spectroscopy on the same day of gelation and after 14 days storage. Measurements were conducted with an IRPrestige-21 FTIR spectrometer (Shimadzu Co., Kyoto, Japan) equipped with an attenuated total reflectance (ATR) accessory, following a method described by Rai and Nitin (2023). Prior to spectral acquisition, baseline correction was applied, and a small amount of oleogel was placed directly onto the diamond ATR crystal. Spectra were recorded in absorbance mode over the wavenumber range of 4000–400 cm^{-1}, with a spectral resolution of 4 cm^{-1} and an average of 128 scans. Spectral processing and analysis were carried out using GraphPad Prism v10 (GraphPad Software, Boston, MA, USA).

2.7. X-ray diffraction (XRD)

A Bruker D8 Advance Eco X-ray diffraction system (Bruker Corp., Billerica, MA, USA) was used to analyze changes in polymorphic form of GMS in the oleogels during storage. Oleogels stored for either 1 or 14 days were transferred onto XRD sample holders and leveled by scraping the surface with a glass microscope slide before placement in the diffractometer. A copper X-ray tube (λ = 1.54 Å) served as the radiation source, operating at 40 kV and 25 mA. Spectra were collected at ambient temperature over a 2θ range of 4–30° using synchronous rotation mode with an acquisition speed of 1.14°/min and a scanning speed of 1 s/step. The instrument was controlled using DIFFRAC COMMANDER software (Bruker Corp.), and peak positions and d-spacing values were analyzed with EVA software (version 4.1.1; Bruker AXS LLC, Madison, WI, USA).

2.8. Statistical analysis

All results are expressed as the mean ± standard deviation (SD), based on replicates (n = 3, unless otherwise mentioned; independently prepared replicates). Statistical analysis was carried out using two-way analysis of variance (ANOVA), followed by Tukey's Honestly Significant Difference (HSD) post hoc test in RStudio (https://www.rstudio.com/), with statistical significance determined using a significance level of α = 0.05. Graphical representations of the data were created using GraphPad Prism version 10 (GraphPad Software, Boston, MA, USA).

3. Results and discussion

3.1. Mechanical stability

To evaluate the stability of the synergistic increase in mechanical strength of EC-GMS binary oleogel systems, an initial trial was conducted using either GMS alone or combinations of EC45 and GMS, formulated to initially have equivalent hardness. Changes in hardness were then evaluated after 1, 14, and 28 days of storage (Fig. 1a). The oleogels structured with GMS alone showed a substantial decline in gel strength, with hardness decreasing significantly after 14 days and stabilizing thereafter with no further notable changes after 28 days. The oleogels prepared with 14% GMS and 2% EC45 (below the CGC of EC45) showed a more gradual reduction in hardness over time. After 14 days, the firmness had declined by nearly 50%, while after 28 days it had further reduced, becoming equivalent to that of the gels structured with GMS alone. In contrast, the oleogel composed of 4% GMS with 10% EC45 (above the CGC of EC45) retained its initial hardness throughout the 28-day period (>20N). By comparison, oleogels structured with 10% EC45 alone were substantially weaker (~10 N; see Fig. 1b), demonstrating retention of oleogel hardness generated by the synergistic interaction between the two compounds. This suggests the formation of a self-supporting polymeric network may play a key role in mitigating the decline in structuring power of GMS and stabilizing gel strength over time.

To test this hypothesis, additional binary oleogels were prepared with 14% GMS and EC45 at concentrations below, at, and above its CGC (2%, 6%, and 10%, respectively). The mechanical strength of these gels was measured after 1 and 14 days of storage, and are shown in Fig. 1b. The oleogel structured solely with GMS completely lost its gelation capacity after 14 days of storage (also confirmed visually; Supporting **data**, Fig. S1). In the binary oleogels, the addition of 2% EC45 produced a significant increase in hardness compared to GMS alone. However, after 14 days storage, there was a significant decrease in hardness. A similar trend was also observed for oleogels containing 6% EC45. However, while the oleogels containing 10% EC45 again showed a significant increase in gel strength (relative to lower EC concentrations), the hardness did not significantly change during storage, indicating full retention of the synergistic interaction between EC and GMS over time. This suggests that a fully self-supporting polymer network provided by the 6% and 10% EC45 (at and above the CGC, respectively) effectively retained the EC-GMS binary oleogel hardness over time. Notably, EC-only oleogels exhibited no significant changes in hardness over the 14-day storage period, indicating that the observed decline in hardness in EC-GMS binary oleogels is primarily associated with GMS rather than EC.

The observed reduction in hardness of single-component GMS oleogels during storage aligns with previous findings (Li et al., 2021; Pakseresht et al., 2023; Zampouni et al., 2022). Consequently, several studies have explored multi-component oleogel systems to address this issue by leveraging cooperative interactions between oleogelators, such as carnauba wax (Pakseresht et al., 2023), phytosterols (Zampouni et al., 2022), or hydroxylated monoglycerides (Li et al., 2024). Whereas previous work primarily focused on mitigating GMS instability, the present study links stability to the synergistic enhancement of the EC-GMS binary oleogelator system.

Based on the results shown in Fig. 1, the retention of EC-GMS synergism during storage can be clearly distinguished between two contrasting structural regimes. In the first scenario, where EC is used below its CGC (e.g., 2% EC45), EC does not form a self-supporting polymer network. Under these conditions, the overall gel structure relies heavily on GMS crystallization for mechanical integrity. As GMS undergoes polymorphic transition and microstructural rearrangement during storage, this dependence results in a measurable decline in hardness. The limited polymer-polymer entanglement and reduced density of junction zones in sub-CGC EC systems provide insufficient structural

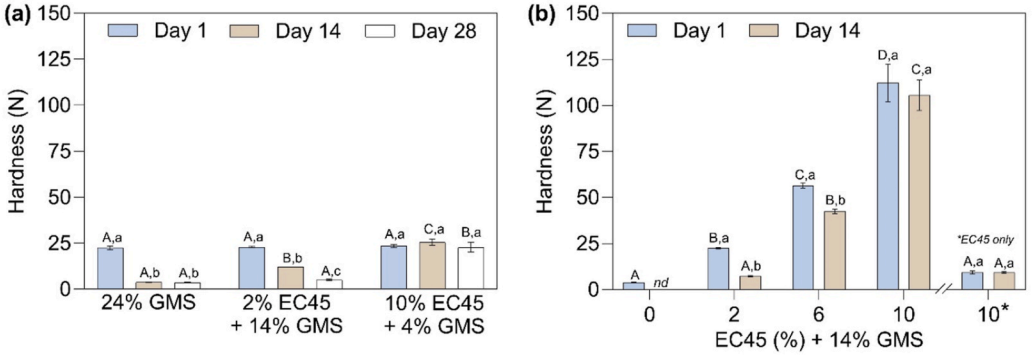

Fig. 1. Changes in oleogel hardness during storage: (a) oleogels with different combinations of glycerol monostearate (GMS) and 45 cP ethyl cellulose (EC45) with equivalent hardness on Day 1; (b) oleogels with 14% GMS alone, and in combination with varying concentrations of EC45. Significant differences ($p < 0.05$) are indicated by different uppercase letters for different oleogels at the same time point, and by different lowercase letters for comparisons of the same formulation at different time points.

reinforcement to stabilize the evolving GMS crystal network. In contrast, in the second scenario, where EC is used at or above its CGC (6% and 10% EC45), a continuous, self-supporting polymer network is established. In this regime, the EC network contributes directly to load-bearing capacity and constrains GMS crystal reorganization. The greater degree of polymer entanglement and increased polymer-polymer contacts enhance mechanical robustness, allowing the synergistically enhanced gel strength to be effectively retained during storage. Thus, the presence of a self-supporting EC network fundamentally alters the structural dependence of the system, shifting it from GMS-dominated structuring to a cooperative, polymer-reinforced architecture. These interaction mechanisms are explored in greater detail in the following section.

3.2. Microstructural properties

Polarized light microscopy (PLM) was used to characterize the impact of storage on the crystalline oleogel network formulated with 14% GMS, both independently and in combination with EC45 (Fig. 2). As the EC polymer network is not visible under polarized light due to the length scale of the polymer chains and the low crystallinity after oleogelation (Davidovich-Pinhas et al., 2014), only changes in the GMS crystalline network are evaluated.

When used alone, the GMS crystal network showed notable differences in morphology and spatial distribution across all formulations over the 14-day storage period. In the single-component oleogel, uniformly distributed spherulitic crystals were evident on Day 1 (Fig. 2a). After 14 days, this single-component oleogel showed aggregation into larger isolated structures and a reduction in the size of crystals within the remaining homogeneous regions (Fig. 2b). These observed crystal morphologies were consistent with previous studies, which have reported both spherulitic crystals shortly after gelation (Rosen-Kligvasser and Davidovich-Pinhas, 2021), and the formation of crystal aggregates during storage (Chen and Terentjev, 2009; Zampouni et al., 2022).

In contrast, the binary oleogels were initially dominated by homogeneously distributed aggregates of needle-like crystals (Fig. 2c–e, g). The transition of GMS crystal morphology from spherulitic to needle-like structures in the presence of EC is consistent with previous reports (Ji and Gravelle, 2025; Sajib et al., 2026). This pronounced morphological shift is attributed to noncovalent interactions between the unsubstituted hydroxyl groups of EC and the polar glycerol headgroups of GMS. Such interactions are thought to facilitate nucleation of GMS crystals along the EC polymer backbone, promoting the formation of aggregated needle-like structures (Ji and Gravelle, 2025). Furthermore, the high miscibility of GMS in triglyceride oils likely supports the synergistic enhancement of gel strength by enabling the growth of these needle-like crystals radiating from numerous nucleation sites into the oil phase (Ji and Gravelle, 2025). Notably, the size of the crystal aggregates appeared to decrease with increasing EC concentration, likely due to the greater availability of interaction sites along the EC backbone that promote more frequent GMS nucleation and the formation of finer needle-like crystals. After 14 days of storage, only minor changes in crystal morphology were observed for the 2% and 6% EC45 formulations, and no substantial alterations were evident in the overall network structure (Fig. 2d–f, h). Although the changes in crystal morphology were subtle, localized regions of crystal aggregation were observed after 14 days of storage. These aggregates were more pronounced in the 2% EC45 formulation and became progressively less evident with increasing EC45 concentration, reaching a minimum at 10% EC45. This trend suggests that EC concentration plays a key role in governing crystal aggregation behavior. Accordingly, the influence of EC concentration on governing molecular level interactions in EC-GMS oleogels is examined and discussed in the following sections.

3.3. Thermal behavior

The impact of EC on the solid-to-liquid thermal transition of GMS in the binary oleogels was monitored throughout the storage period using DSC. Thermograms of oleogels prepared with 14% GMS and EC45 at concentrations below, at, and above its CGC are presented in Fig. 3.

In the single-component GMS oleogel, the thermal behavior immediately after crystallization (Day 0) showed two distinct melting events with peak melting temperatures (T_m) occurring at ~38 °C and ~60 °C (Fig. 3a) which correspond to the metastable sub-α and inverse lamellar (Lα) polymorphs, respectively (Rondou et al., 2025). At Day 1, these peaks were no longer present, and only a singular, intense melting event was present with a T_m of ~70 °C, indicative of the more stable β-polymorph (Prodromidis et al., 2023; Vereecken et al., 2009). After 14 days of storage, a nearly identical melting profile was observed, with only a slight increase in T_m of the β-polymorphic peak to ~72 °C.

For the binary oleogels, the Day 0 melting profiles mirrored that of the single-component system, irrespective of EC45 concentration, with only the sub-α- and Lα-polymorphs present (Fig. 3b–d); however, differences became apparent upon storage. On Day 1, the sub-α and Lα peaks were still present, but had reduced intensity relative to Day 0. After 14 days, the peaks corresponding to both the sub-α- and Lα polymorphs were no longer present in the binary oleogels with 2% EC45 but were still observed (with further reduced intensity) in those containing 6% and 10% EC45. The β polymorph was also apparent, but similarly with a reduced intensity relative to the single-component oleogel, indicating the transition to the β-form was incomplete.

The thermal response in Fig. 3 clearly demonstrates that the presence of an EC network slows the sub-α to β polymorphic transition of GMS during storage, a behavior previously reported for monoglyceride

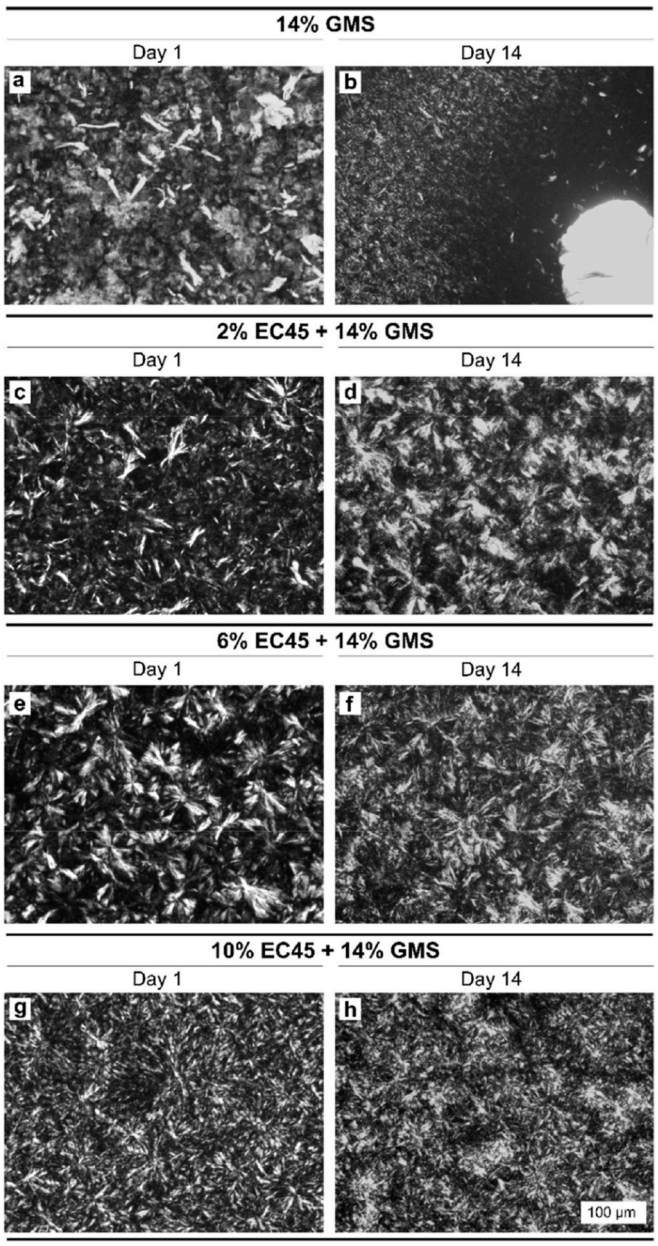

Fig. 2. Polarized light microscopy images of oleogels with 14% glycerol monostearate (GMS) alone (a-b) and in combination with 45 cP ethyl cellulose (EC45) at concentrations below (2%, c-d), at (6%, e-f), and above (10%, g-h) the critical gelation concentration (CGC) of EC45, showing changes in GMS crystal arrangements during storage.

oleogels prepared with EC (Lopez-Martínez et al., 2015). Although the enthalpy of the sub-α peak was comparable across all formulations at Day 0 (~3 J/g), differences became evident over time (Supporting **Data**; Table S1). By Day 1, no enthalpy was recorded for the single-component GMS oleogel, whereas binary systems retained measurable values that decreased with increasing EC concentration (~2 J/g at 2% EC45 to ~1 J/g at 10% EC45). After 14 days, the sub-α was not present in the 2% EC45 system, while binary oleogels containing 6% and 10% EC45 still showed residual enthalpies of ~0.5-0.7 J/g. These results align with the observed reduction in GMS crystal aggregation (Fig. 2), supporting that microstructural changes arising from EC-GMS interactions accompany the delayed sub-α to β transition. Overall, the data confirm that the higher concentration of EC aids in delaying the sub-α to β polymorphic transition, which can be attributed to a greater number of GMS-EC interactions.

3.4. Molecular interactions

FTIR analysis was used to investigate the time-dependent changes in the molecular interactions of both the single-component and binary EC-GMS oleogels (Fig. 4). To investigate the intermolecular interactions that are initially formed in the EC-GMS oleogels which may contribute to the observed synergy, FTIR analysis was conducted on Day 0 and after 2 weeks storage (Day 14).

While previous studies characterizing EC-GMS binary oleogels have proposed hydrogen bonding may contribute to the observed synergistic behavior, there has been scarce direct evidence to support this (Davidovich-Pinhas et al., 2015). Specifically, because the O-H stretching band of EC is difficult to detect, the contribution of EC-GMS hydrogen bonding to the binary oleogels has remained relatively speculative (Wang et al., 2026; Zhang et al., 2022). However, Fig. 4a shows that in the present work, this band was clearly visible in the single-component EC oleogels, centering around ~3475 cm^{-1}, thus allowing for direct evaluation of the EC-GMS hydrogen bonding interactions. Notably, this band (and the overall spectra of the EC oleogels) did not change over the 2-week storage period.

In contrast, the 14% GMS oleogels displayed a very broad O-H stretching band (~3100-3550 cm^{-1}) with a central peak at ~3305 cm^{-1} and two distinct shoulders apparent on either side of this maximum. This band pattern is consistent with previous reports (Zampouni et al., 2022) and has been attributed to the sub-α form of GMS. The central peak has been attributed to hydrogen bonding between the 3-OH group of the glycerol (i.e., in the sn-3 position). It has been proposed that this group has a higher intensity in the sub-α form due to its higher conformational freedom relative to the 2-OH group (shoulder at ~3230 cm^{-1}), allowing it to hydrogen bond more easily with neighboring C=O groups (Chen and Terentjev, 2009). Thus, the FTIR O–H stretching spectra on Day 0 was consistent with the sub-α form, which aligns with the thermal analysis of the fresh GMS oleogels (Fig. 3).

In the binary oleogels, as EC content increased, the intensity of the GMS bands gradually reduced, and the shoulders became less apparent. The EC O-H stretching band also appeared to be superimposed with the GMS OH stretching band. Therefore, to isolate the impact of EC on the GMS spectra, the signal from the 10% EC-only oleogel spectra was subtracted from the EC-GMS spectra, with intensity scaled for EC concentration (Fig. 4b, difference spectra denoted by Δ). With increasing EC content, a decrease in overall band intensity and a shift in the O-H stretching peak position to higher wavenumbers was observed, with maximum peak intensity at ~3350 cm^{-1} with 10% EC45. This shift in the peak position (~45 cm^{-1}) indicates the presence of EC alters the O-H stretching interaction for a portion of the total GMS population, which can be attributed to an increasing population of GMS molecules forming hydrogen bonds with the EC network. This progressive shift in the central peak suggests the EC-GMS hydrogen bonding occurs primarily with the 3-OH group of GMS due to its higher conformation freedom and lower steric hindrance (Chen et al., 2009). EC-GMS hydrogen bonds may initially form in the liquid state and serve as nucleation sites for crystallization, producing crystal edges at the polymer backbone, and allowing the interactions to persist in the solid state. This observation aligns with the dramatic change in crystal morphology of GMS in the presence of EC (Fig. 2) and the depression in the crystallization temperature reported previously (Sajib et al., 2026). A shift in the C=O of the GMS ester group was also observed (from ~1730 cm^{-1} for GMS alone to ~1740 cm^{-1} for GMS with 10% EC45). However, due to the presence of an analogous distinct peak in the EC45-only oleogel at 1745 cm^{-1}, this apparent shift was likely due to peak overlap and cannot be unambiguously associated with a perturbation in the GMS hydrogen bonding.

After 2 weeks of storage, the oleogels structured only with GMS exhibited pronounced spectral changes in peaks associated with

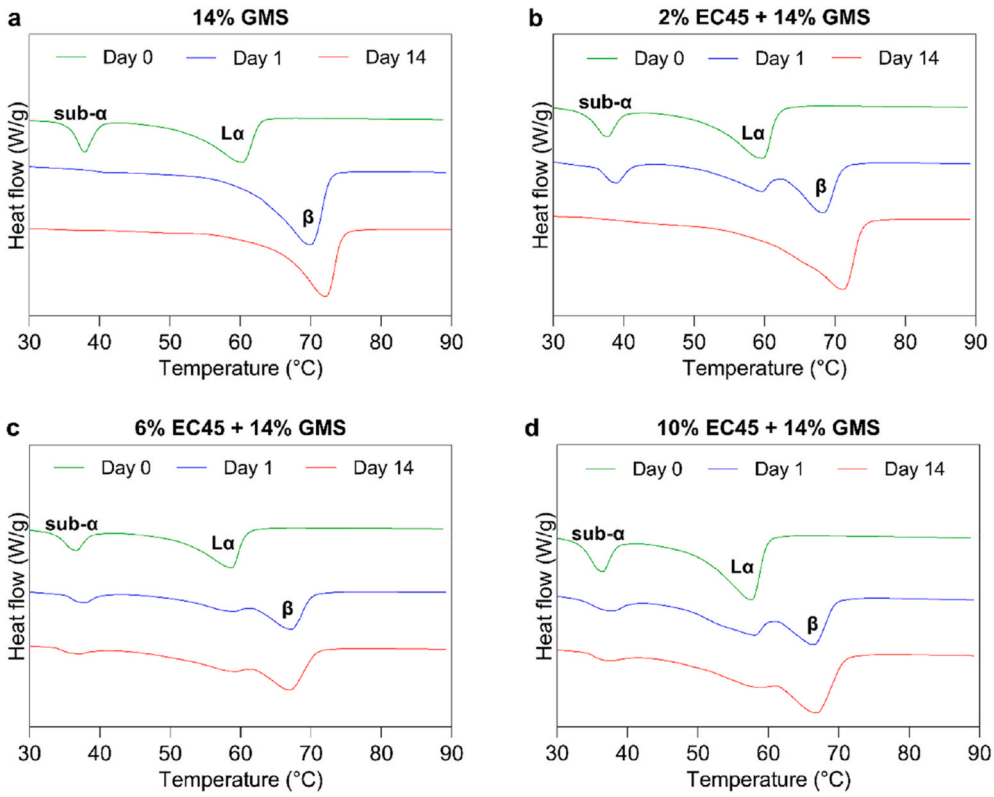

Fig. 3. Thermograms of oleogels with 14% glycerol monostearate (GMS) alone (a) and in combination with 45 cP ethyl cellulose (EC45) at concentrations below (2%, b), at (6%, c), and above (10%, d) the critical gelation concentration (CGC) of EC45, showing time-dependent changes in GMS polymorphism during storage.

hydrogen bonding (Fig. 4c). A direct comparison between spectra collected on Day 1 and Day 14 is also provided as supporting information (Supporting **data**, Fig. S2). The observed changes included splitting of the carbonyl peak into two distinct bands centered around ~1730 cm^{-1}. Distinct differences in intensity throughout the fingerprint region were also observed, including those associated with C–O stretching (~1200-1000 cm^{-1}), and a loss of the doublet peak associated with aliphatic chain packing centered around ~720 cm^{-1} also occurred during storage.

However, the most notable change was seen in the O–H stretching band (3200–3600 cm^{-1}). After storage, the peaks associated with both the 3-OH and 2-OH glycerol groups (~3305 cm^{-1} and ~3230 cm^{-1}, respectively) were approximately equivalent in intensity, while the shoulder at higher wavenumbers was not apparent. These changes are consistent with that reported previously for monoglyceride-based oleogels during storage (Chen and Terentjev, 2009; Zampouni et al., 2022). It has been reported that the change in relative intensity of the 3-OH and 2-OH bands is due to the sub-α to β polymorphic transition and can be attributed to the higher packing density of the β-form (Alfutimie et al., 2014; Chen et al., 2009; Zampouni et al., 2022). With increasing EC content, both the decrease in band intensity and gradual shift in peak position for both peaks was observed (Fig. 4d, EC band subtracted). This shift to higher wavenumbers was consistent with that seen for the sub-α form but was smaller in magnitude (~6 cm^{-1}), which may indicate fewer or weaker EC-GMS interactions after the transition to the β form.

The splitting of the C=O band into a doublet upon storage can also be attributed to changes in the hydrogen bonding upon transforming from the sub-α to β form, as this band has been attributed to carbonyl/hydroxyl hydrogen bonding of GMS (Chen and Terentjev, 2009). Thus, the change in the local chemical environment likely differs between the 3-OH and 2-OH glycerol groups, giving rise to the observed doublet. There were also progressive changes in the C=O band, where the lower wavenumber doublet (~1730 cm^{-1}) decreased in intensity, and the higher wavenumber doublet (~1740 cm^{-1}) broadened. The latter can be attributed to overlap with the C=O band apparent in the EC-only oleogels resulting from the liquid oil phase. No apparent shift in the alkyl chain packing band at ~720 cm^{-1} was observed in the presence of EC, indicating EC does not perturb the chain packing, consistent with that observed for the sub-α form.

Due to the overall decrease in band intensity in the presence of EC and the consistency of O-H stretching band peak positions in the sub-α and β form, the persistence of the sub-α form could not be unambiguously determined from the FTIR spectra. Further, the coexistence of both polymorphs are also difficult to discern due to these factors. However, to the best of our knowledge, these results are the first direct evidence demonstrating changes in the GMS hydrogen bonding interactions when crystallized in the presence of EC. The shift in both the 3-OH and 2-OH bands in the β-form also suggests this hydrogen bonding persists after the sub-α to β transition, which may further contribute to the retention in synergistic enhancement after storage.

3.5. *Polymorphic behavior*

To further examine the polymorphic forms of GMS crystals over time, XRD analysis was performed on single-component and binary oleogels structured with 14% GMS after 1 and 14 days of storage (Fig. 5). On Day 1, the single-component GMS oleogel showed a number of distinct wide-angle peaks, including partially overlapping peaks with d-spacings of ~4.55 Å and ~4.50 Å, and distinct peaks with d-spacings of ~4.4 Å, ~4.3 Å, ~3.95 Å, ~3.9 Å, ~3.8 Å and ~3.65. These peaks have all been previously attributed to the β-polymorph (Vereecken et al., 2009). Notably, there was no peak with an associated d-spacing of ~4.2 Å. This peak is characteristic of the sub-α polymorph, as it is caused by the hexagonal packing of the in-plane glycerol headgroups (Chen et al., 2009), while additional peaks associated with the sub-α form have been shown to overlap with those arising from the β polymorph. As this same

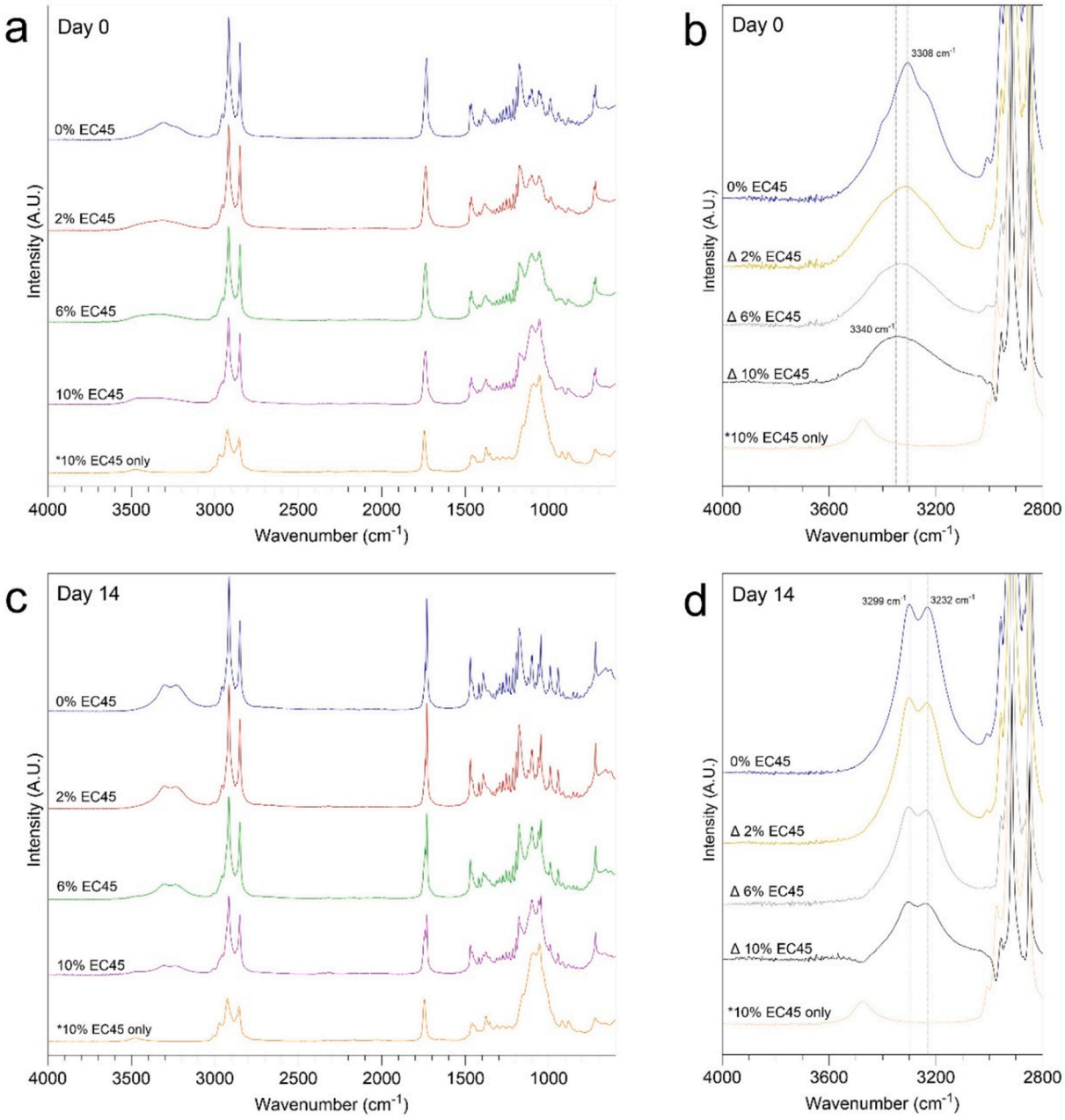

Fig. 4. FTIR spectra of oleogels with 14% glycerol monostearate (GMS) alone and in combination with 45 cP ethyl cellulose (EC45) at varying concentrations on Day 0 (a,b) and Day 14 (c,d) of storage. The hydrogen-bonding band is highlighted in (b,d), which depicts the binary EC-GMS oleogels after subtracting the EC spectra, as denoted by the symbol Δ.

peak pattern was maintained after 14 days of storage, the XRD spectra indicates the GMS oleogels had transitioned from the sub-α to the β-form by Day 1, consistent with the thermal behavior observed by DSC (Fig. 3). This transition to the β-form is also consistent with earlier studies (Chen and Terentjev, 2009; Heymans et al., 2018; Li et al., 2021; Lopez-Martínez et al., 2015; Paksereshet al., 2023; Rondou et al., 2022).

In the binary oleogel structured with 2% EC45, the peaks associated with the β polymorph were also observed on Day 1. However, a distinct peak with a d-spacing of ~4.17 Å was also present, indicating that a portion of the GMS remained in the sub-α form (Fig. 5b). On Day 14, both the sub-α and β peaks persist, but the former has a notably reduced intensity relative to the β peaks, suggesting more of the GMS transitioned to the β form during storage, but the process was not complete. This is again consistent with the DSC profiles, where the sub-α endotherms were present, but with a smaller enthalpy. The sub-α peaks were also observed in the binary oleogels with 6% and 10% EC45, also indicating the persistence of a minor GMS population in the sub-α form after 14 days of storage, consistent with the corresponding DSC thermograms (Fig. 5c and d). Were observed, similar to the trend in the GMS-only oleogel. Overall, the XRD results suggest that although β crystal polymorphs formed during storage, the presence of a self-supporting EC network delayed the sub-α to β polymorphic transition. This aligns with the retention of oil structuring power in the EC-GMS binary oleogel systems, which is correlated to the retention in the synergistic enhancement in gel strength.

The polymorphic transition of GMS during storage is driven by thermodynamic stabilization, whereby metastable sub-α crystals reorganize toward the more stable β form as molecular packing becomes more ordered (Rondou et al., 2025; Wang and Marangoni, 2014). This solid-solid polymorphic transition can proceed gradually at ambient

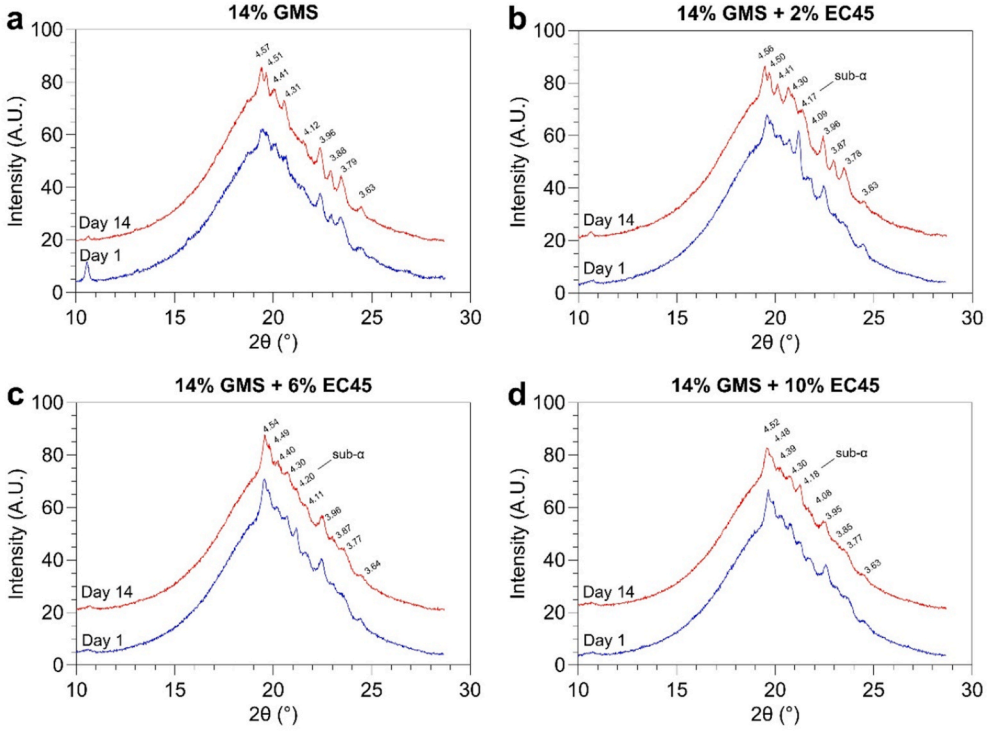

Fig. 5. X-ray diffraction patterns of oleogels with 14% glycerol monostearate (GMS) alone (a) and in combination with either 2% (b), 6% (c) or 10% (d) ethyl cellulose (EC45) during storage. The numbers above the diffraction patterns indicate the corresponding d-spacing values.

temperature, consistent with time-dependent structural evolution reported for GMS/monoglyceride-based systems (Rondou et al., 2025; Wang et al., 2026). Because lipid polymorphism is closely tied to changes in chain packing and noncovalent interactions (including dispersion/van der Waals contributions), improved packing provides a key driving force for the β form (Balcázar-Zumaeta et al., 2026; Wagner and Davidovich-Pinhas, 2023). As the delayed polymorphic change was seen in all EC-GMS binary oleogels, the EC-GMS intermolecular interactions (e.g., hydrogen bonding observed by FTIR) are likely the main driver in delaying this transition. However, increasing EC content may also limit mass transfer, which could likely further delay this process, leading to a higher retention in gel strength over time.

3.6. Effect of EC/GMS ratio on mechanical strength

To further assess how GMS concentration influences the storage stability of binary EC-GMS oleogels, formulations were prepared with varying GMS levels while maintaining EC45 at its CGC (6%) (Fig. 6). A significant reduction in oleogel hardness after 14 days of storage was observed in formulations containing ≤8% GMS (with the exception of 4% GMS), whereas formulations with ≥10% GMS showed no significant changes in hardness over the same period. For the 4% GMS system, the modest change in hardness can be attributed to the low GMS concentration, resulting in the observed modest decrease. While this effect was not significant, it may suggest that the EC/GMS ratio in this formulation was insufficient to sustain the synergistic effect during storage. The reductions in hardness observed for the 6% and 8% GMS formulations further indicate limited effectiveness in maintaining these synergistic interactions over time. In contrast, the retention of hardness in the 10% and 12% GMS formulations demonstrates effective preservation of the synergistic enhancement in gel strength throughout the 14-day storage period.

The observed stability in oleogel hardness over the 14-day storage period for formulations containing ≥10% GMS may be attributed to the combined network density provided by both EC and GMS. At the CGC

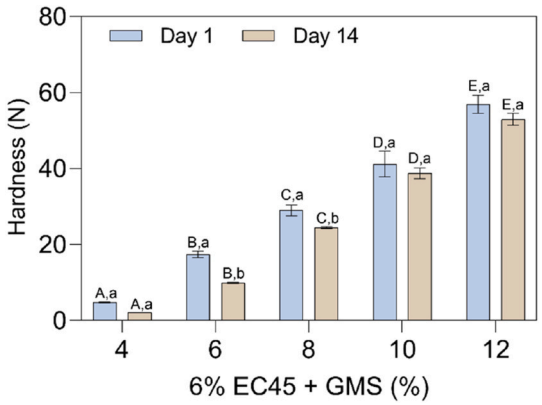

Fig. 6. Effect of EC/GMS ratio on the retention of synergistic effect over 14 days of storage. Significant differences ($p < 0.05$) are indicated by different uppercase letters for oleogel formulations within the same day, and by different lowercase letters for comparisons over time for the same formulation.

(6% EC45), the system-spanning EC network entraps the liquid oil phase in discrete pockets, while also providing a 3-dimensional scaffold of interaction sites for GMS to heterogeneously nucleate. With increasing GMS content, the crystal network density within the entangled polymer network becomes more dense, and the greater number of polymer-crystal and crystal-crystal interactions help stabilize GMS crystals in the sub-α form, thereby preserving the associated enhancement in mechanical strength. We thus propose the metastable sub-α crystal form is kinetically stabilized by the polymer-crystal intermolecular interactions. An increase in the density of EC-GMS interactions (via increasing EC content) would thus be expected to reduce the probability of crystals able to overcome the energetic barrier necessary to initiate the sub-α to β polymorphic transition, as well as limit mass transport within the network, thus limiting the growth or aggregation of β form crystals, limiting micro-scale structural reorganization, and ultimately helps

preserve mechanical integrity during storage. Overall, in addition to forming a self-supporting EC network, achieving sufficient network connectivity is essential for maintaining the long-term structural stability of EC-GMS binary oleogels during storage. This connectivity depends not only on the absolute concentrations of the individual components but also on their relative EC-to-GMS ratio.

4. Conclusion

The synergistic interaction between ethyl cellulose (EC) and glycerol monostearate (GMS) in binary oleogel systems results in a multiplicative increase in hardness compared to the corresponding single-component systems. This study reports, for the first time, on the storage stability of this synergistic interaction. A reduction in this synergistic effect over time was associated with the sub-α to β polymorphic transition of GMS, which led to microstructural rearrangement and a decline in mechanical strength, particularly in single-component GMS oleogels. In binary EC-GMS systems, although partial polymorphic transition occurred during storage, mechanical strength was largely preserved, with stability governed by whether EC was used at or above its critical gelation concentration (CGC) and by the EC/GMS ratio. FTIR, DSC, and XRD analyses consistently demonstrated that the presence of a self-supporting EC network (formed at 6% and 10% EC45) delayed the polymorphic transition of GMS during 14 days of storage at 22 °C. Microstructural analysis further revealed reduced β-crystal aggregation in these formulations over time. The findings further indicated that, beyond establishing a self-supporting EC network, maintaining a critical crystalline density is essential to preserve EC-GMS synergistic effect during storage. Future studies investigating how various compositional factors contribute to the kinetics of the GMS polymorphic transition may be helpful to enable further leveraging the benefits of EC-GMS synergistic interactions in producing stable EC-GMS binary oleogels. Overall, these findings establish a foundation for designing stable EC-GMS binary oleogels, whereby strategically leveraging their synergistic interaction can significantly enhance gelator efficiency and enable potential cost reductions in fat-mimetic production. Moreover, the complementary functional properties of EC and GMS may also provide greater formulation flexibility, supporting the development of functional oleogels for a broad range of fat-mimetic applications, such as for alternative protein-based food applications.

Declaration of competing interest

The authors declare the following financial interests/personal relationships which may be considered as potential competing interests: Andrew J. Gravelle reports financial support was provided by UC Davis Integrative Center for Alternative Meat and Protein (iCAMP). Mursalin Sajib reports financial support was provided by Swedish Research Council Formas. Nitin reports financial support was provided by National Institute of Food and Agriculture. If there are other authors, they declare that they have no known competing financial interests or personal relationships that could have appeared to influence the work reported in this paper.

Acknowledgements

The authors would like to thank James Fettinger and Rajesh Kandel for their assistance with the XRD analysis, Gaby Hidayat for assisting with microscopy and large deformation mechanical analyses, and Samantha Chin for assisting with FTIR analysis. Financial support was provided by Formas – the Swedish Research Council for Sustainable Development [grant number 2022-02804], the Sustainable Agricultural Systems program of USDA-NIFA [grant number 2021-699012-35978], and the UC Davis Integrative Center for Alternative Meat and Protein (iCAMP) [grant number ICAMP-0011], all of which are gratefully acknowledged.

Appendix A. Supplementary data

Supplementary data to this article can be found online at https://doi.org/10.1016/j.crfs.2026.101421.

References

Alfutimie, A., Curtis, R., Tiddy, G.J., 2014. Gel phase (Lβ) formation by mixed saturated and unsaturated monoglycerides. Colloids Surf. A Physicochem. Eng. Asp. 456, 286–295.
Balcázar-Zumaeta, C.R., Chagas-Júnior, G.C.A., Ferreira, N.R., Pinheiro, W.B.D.S., Maicelo-Quintana, J.L., Cayo-Colca, I.S., Castro-Alayo, E.M., 2026. Advances in cocoa butter and alternative fats: composition and crystallization dynamics in chocolate production. Eur. Food Res. Technol. 252 (3), 107.
Bin Sintang, M.D., Danthine, S., Brown, A., Van de Walle, D., Patel, A.R., Tavernier, I., Rimaux, T., Dewettinck, K., 2017. Phytosterols-induced viscoelasticity of oleogels prepared by using monoglycerides. Food Res. Int. 100, 832–840.
Chen, C., Van Damme, I., Terentjev, E., 2009. Phase behavior of C18 monoglyceride in hydrophobic solutions. Soft Matter 5 (2), 432–439.
Chen, C., Terentjev, E., 2009. Aging and metastability of monoglycerides in hydrophobic solutions. Langmuir 25 (12), 6717–6724.
Davidovich-Pinhas, M., Barbut, S., Marangoni, A.G., 2014. Physical structure and thermal behavior of ethylcellulose. Cellulose 21 (5), 3243–3255.
Davidovich-Pinhas, M., Barbut, S., Marangoni, A.G., 2015. The role of surfactants on ethylcellulose oleogel structure and mechanical properties. Carbohydr. Polym. 127, 355–362.
García-Ortega, M.L., Charó-Alvarado, M.E., Pérez-Martínez, J.D., Toro-Vazquez, J.F., 2024. Thermomechanical characterization of oleogels elaborated with a low molecular weight ethyl cellulose and monoglycerides. Food Biophys. 1–18.
Giacomozzi, A.S., Carrín, M.E., Palla, C.A., 2018. Muffins elaborated with optimized monoglycerides oleogels: from solid fat replacer obtention to product quality evaluation. J. Food Sci. 83 (6), 1505–1515.
Gravelle, A.J., 2024. Direct oil structuring using ethylcellulose. In: Advances in Oleogel Development, Characterization, and Nutritional Aspects. Springer, pp. 157–175.
Haj Eisa, A., Laufer, S., Rosen-Kligvasser, J., Davidovich-Pinhas, M., 2020. Stabilization of ethyl-cellulose oleogel network using lauric acid. Eur. J. Lipid Sci. Technol. 122 (2), 1900044.
Heymans, R., Tavernier, I., Danthine, S., Rimaux, T., Van der Meeren, P., Dewettinck, K., 2018. Food-grade monoglyceride oil foams: the effect of tempering on foamability, foam stability and rheological properties. Food Funct. 9 (6), 3143–3154.
Hu, L., Zhang, R., Song, S., Han, Z., Ziao, Z., Shao, J.-.H., 2025. The synergistic effects of oleogelators based on different structuring mechanisms: a viable way to tailor oleogels with ideal thermo-responsiveness and rheological properties. Food Chem. 479, 143820.
Ji, L., Gravelle, A.J., 2025. Modulating the behavior of ethyl cellulose-based oleogels: the impact food-grade amphiphilic small molecules on structural, mechanical, and rheological properties. Food Hydrocoll. 159, 110703.
Li, J., Guo, R., Bi, Y., Zhang, H., Xu, X., 2021. Comprehensive evaluation of saturated monoglycerides for the forming of oleogels. Lwt 151, 112061.
Li, J., Xiao, Y., Guo, R., Bi, Y., Zhang, H., Xu, X., 2024. Enhancing the long-term stability of glyceryl monostearate-based oleogels by incorporating hydroxy monoglyceride as an additional scaffolding agent. Lwt 214, 117154.
Lopez-Martínez, A., Charó-Alonso, M.A., Marangoni, A.G., Toro-Vazquez, J.F., 2015. Monoglyceride organogels developed in vegetable oil with and without ethylcellulose. Food Res. Int. 72, 37–46.
Pakseresht, S., Tehrani, M.M., Farhoosh, R., Koocheki, A., 2023. The monoglyceride oleogel characteristics modified by carnauba wax. Lwt 185, 115156.
Pakseresht, S., Mazaheri Tehrani, M., 2022. Advances in multi-component supramolecular oleogels-a review. Food Rev. Int. 38 (4), 760–782.
Palla, C., Giacomozzi, A., Genovese, D.B., Carrín, M.E., 2017. Multi–objective optimization of high oleic sunflower oil and monoglycerides oleogels: searching for rheological and textural properties similar to margarine. Food Struct. 12, 1–14.
Palla, C.A., Dominguez, M., Carrín, M.E., 2022. An overview of structure engineering to tailor the functionality of monoglyceride oleogels. Compr. Rev. Food Sci. Food Saf. 21 (3), 2587–2614.
Prodromidis, P., Biliaderis, C.G., Katsanidis, E., Moschakis, T., 2023. Effect of Tween 20 on structure, phase-transition behavior and mechanical properties of monoglyceride oleogels. Food Struct. 38, 100345.
Rai, R., Nitin, N., 2023. Apple-derived 3D scaffold for improving gastrointestinal viability and in-situ growth of probiotics. Food Res. Int. 168, 112758.
Rondou, K., De Witte, F., Dewettinck, K., Van Bockstaele, F., 2025. Effect of shear on polymorphic transitions in monoglyceride oleogels. Crystals 15 (6), 495.
Rondou, K., De Witte, F., Rimaux, T., Dewinter, W., Dewettinck, K., Verwaeren, J., Van Bockstaele, F., 2022. Multiscale analysis of monoglyceride oleogels during storage. J. Am. Oil Chem. Soc. 99 (11), 1019–1031.
Rosen-Kligvasser, J., Davidovich-Pinhas, M., 2021. The role of hydrogen bonds in TAG derivative-based oleogel structure and properties. Food Chem. 334, 127585.
Sajib, M., Nitin, N., Gravelle, A.J., 2026. Role of ethyl cellulose polymer network on synergistic enhancement of glycerol monostearate and ethyl cellulose binary oleogels. Food Hydrocoll. 179, 112755.
Sivakanthan, S., Fawzia, S., Madhujith, T., Karim, A., 2022. Synergistic effects of oleogelators in tailoring the properties of oleogels: a review. Compr. Rev. Food Sci. Food Saf. 21 (4), 3507–3539.

Soleimanian, Y., Ghazani, S.M., Marangoni, A.G., 2024. Ethylcellulose oleogels of oil glycerolysis products as functional adipose tissue mimetics. Food Hydrocoll. 151, 109756.
Vereecken, J., Meeussen, W., Foubert, I., Lesaffer, A., Wouters, J., Dewettinck, K., 2009. Comparing the crystallization and polymorphic behaviour of saturated and unsaturated monoglycerides. Food Res. Int. 42 (10), 1415–1425.
Wagner, K., Davidovich-Pinhas, M., 2023. Di-acylglycerides as oil structuring agents. Food Struct. 36, 100320.
Wang, G., Zhao, H., Tao, H., Kang, X., Yu, B., Cui, B., 2026. Synergistic interactions of ethyl cellulose and glycerol monostearate in composite oleogel systems. J. Food Meas. Char. 20, 3094–3108.
Wang, F.C., Marangoni, A.G., 2014. Nature and dynamics of monostearin phase transitions in water: stability and the sub-α-gel phase. RSC Adv. 4 (92), 50417–50425.
Woern, C., Marangoni, A.G., Weiss, J., Barbut, S., 2021. Effects of partially replacing animal fat by ethylcellulose based organogels in ground cooked salami. Food Res. Int. 147, 110431.
Zampouni, K., Soniadis, A., Moschakis, T., Biliaderis, C.G., Lazaridou, A., Katsanidis, E., 2022. Crystalline microstructure and physicochemical properties of olive oil oleogels formulated with monoglycerides and phytosterols. Lwt 154, 112815.
Zetzl, A.K., Marangoni, A.G., Barbut, S., 2012. Mechanical properties of ethylcellulose oleogels and their potential for saturated fat reduction in frankfurters. Food Funct. 3 (3), 327–337.
Zhang, J., Zhang, M., Chen, K., Deng, D., 2025. Improvement strategies for fats and oils used in future food processing based on health orientation and sustainability: research progress, challenges and solutions. Crit. Rev. Food Sci. Nutr. 65 (1), 47–63.
Zhang, R., Zhang, Y., Yu, J., Gao, Y., Mao, L., 2022. Rheology and tribology of ethylcellulose-based oleogels and W/O emulsions as fat substitutes: role of glycerol Monostearate. Foods 11, 2364.